

Coincidence Detection for Neutron Activation Analysis

senior thesis

Patricia J Lee

Advisor: Prof. Robert McKeown

May 2000

Acknowledgement

There are many people without whom this project would not have been possible. First, I would like to thank my advisor, Robert McKeown, for offering me the opportunity to work on this project. I would especially like to thank Bryan Tipton for the enormous amount of help he has given me. I also acknowledge the assistance from other members of Caltech's KamLAND group, Andreas Piepke, K.B. Lee, and Petr Vogel. Thanks to Takeyasu Ito for his assistance in setting up MIDAS. I also appreciate the help I have received from Tim Barker in the shop and from Emma Huang for lending her strength in the construction of the detector shielding.

I would also like to thank my friends and family for the help and support they have given me. Very special thanks to my roommates, Helen Claudio and Vidya Bhalodia, for technical assistance in writing this thesis. I would also like to thank Dominic Lucchetti for his expertise in computers. To those people: Meep!

Contents

1	Purpose	4
2	Physics	5
2.1	Motivation	5
2.2	Neutron Activation Analysis	6
2.3	Coincidence Detection	7
2.3.1	Shielding	8
3	Experimental Setup	9
3.1	Overview	9
3.2	Photomultiplier Tube	9
3.3	High Purity Germanium Photon Detector	10
3.4	Electronics	11
3.5	Data Acquisition	12
4	Data Analysis	13
4.1	Shielding Effects on the HPGe Detector	13
4.2	PMT Calibration from Compton Scattering	13
4.3	HPGe Detector Calibration	16
4.4	HPGe Detector Resolution	17
4.5	Efficiency of the HPGe detector	17
4.6	TDC Calibration	21
4.7	Na Coincidence Measurement	24

4.8	Expected Background Counts	26
5	Results and Conclusion	31
5.1	Expected Counting Rate	31
5.2	Sensitivity of the Coincidence Setup	32
5.3	Future Improvements	33
5.4	Conclusion	33

Chapter 1

Purpose

A new large neutrino detector called KamLAND (Kamioka Liquid scintillator Anti-Neutrino Detector) is currently being constructed in the underground site in Japan that used to be the home of the Kamiokande experiment. The principal goal of this international collaboration will be to investigate neutrino oscillations by studying the flux and energy spectra of neutrinos produced by nuclear reactors in Japan. KamLAND will also be measuring solar neutrinos in an effort to solve the solar neutrino deficit puzzle. In addition, it is possible to extract the ratio of uranium to thorium in the crust and mantle of the Earth from the background of the reactor neutrino spectra[1].

To achieve high precisions in the measurements, KamLAND must first minimize its background signals. The collaborators at Caltech have been involved in measuring the radioactivity of the materials used in constructing the detector. Gamma sources in the materials are typically detected by placing them next to a Germanium detector in a well-shielded box. However, as will be shown in the next section, conventional detectors can not achieve the level of sensitivity necessary to detect the small amounts of radioactivity allowed in the KamLAND scintillator. The purpose of this thesis project is to design and build a coincidence setup that will be able to measure the radioactivity of the liquid scintillator at KamLAND using Neutron Activation Analysis of an irradiated sample.

Chapter 2

Physics

2.1 Motivation

The radiopurity required for the liquid scintillator at KamLAND is 10^{-14} g/g for ^{238}U , ^{232}Th , and ^{40}K for the reactor experiment. The amount radioactive material remaining in a sample after time t is

$$x(t) = x_0 2^{-t/\tau_{1/2}},$$

where x_0 is the initial amount of radioactive material in the sample and $\tau_{1/2}$ is the half-life. If we take the derivative of the function

$$\frac{dx(t)}{dt} = -\frac{x_0}{\tau_{1/2}} (\ln 2) 2^{-t/\tau_{1/2}}.$$

Assume that our sample contains 10^{-14} g/g of each of these radioactive elements, and we would like to detect at least 1 decay per day from ^{238}U , ^{232}Th , and ^{40}K . Then

$$\frac{dx(1\text{day})}{dt} = -\frac{x_0}{\tau_{1/2}} (\ln 2) 2^{-1/\tau_{1/2}} = 1,$$

with $\tau_{1/2}$ in units of day. Therefore the amount of radioactive material we need initially is

$$x_0 = \tau_{1/2} 2^{1/\tau_{1/2}} / \ln 2.$$

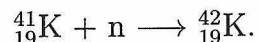
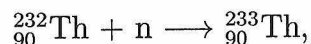
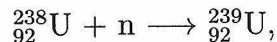
	^{239}U	^{233}Th	^{42}K
half-life	$4.5 \times 10^9 \text{ y}$	$1.4 \times 10^{10} \text{ y}$	$1.3 \times 10^9 \text{ y}$
number of atoms needed for detection	2.4×10^{12}	7.4×10^{12}	6.9×10^{11}
amount of sample required	94 kg	280 kg	$4.6 \times 10^{-4} \text{ kg}$

Even if we assume our detector is functioning at 100% efficiency and ignore the background, it still requires 280 kg of liquid scintillator in the detector in order to measure 1 decay per day from each one of these isotopes. This is simply not a realistic approach to the problem. Therefore, we must seek alternative methods to make the measurements.

2.2 Neutron Activation Analysis

NAA is often used in detecting small traces of radioactivity in materials. The idea is to irradiate the sample in a nuclear reactor to produce different isotopes of the elements that are being detected. If the isotopes produced have a shorter half-life than the original isotopes, the radioactivity will increase to a level which conventional detectors can measure. The original concentration of the radioactive elements can then be inferred from the measurements of the new isotopes and their daughter isotopes.

For this experiment, we are interested in ^{238}U , ^{232}Th , and ^{40}K , since they have the largest natural abundance. If we bombard these isotopes with neutrons, the following reactions occur:



We use the reaction for ^{41}K instead of ^{40}K because ^{41}K is the stable isotope. In nature, ^{41}K accounts for 99.99% of the potassium isotopes and ^{40}K accounts for 0.01107%. Therefore it would be easier to measure the concentration of ^{41}K in the sample and use the results to determine the concentration of ^{40}K assuming the ratio of their occurrence is the same as in nature.

2.3 Coincidence Detection

Once the sample has been irradiated, it will take a few days to transport it from the reactor site to the laboratory where the detector is. Due to the short half-lives of ^{239}U and ^{233}Th , we can only observe the decays of their respective daughter isotopes ^{239}Np and ^{233}Pa in our detector.

isotope	half-life	daughter isotope	half-life of daughter
$^{239}_{92}\text{U}$	23.5 m	$^{239}_{93}\text{Np}$	2.35 d
$^{233}_{90}\text{Th}$	22.3 m	$^{233}_{91}\text{Pa}$	27.0 d
$^{42}_{19}\text{K}$	12.4 h	$^{42}_{20}\text{Ca}$	stable

^{239}Np , ^{233}Pa , and ^{42}K each undergoes β decay, and the daughter isotopes subsequently emit photons of specific energies. Therefore we can dissolve the irradiated sample in liquid scintillator and use a photomultiplier tube (PMT) to detect scintillation light as the β^+ particles annihilate. We correlate the signals from the PMT and the germanium detector and look for coincidences. In the case of ^{239}Np decay, there is a 192 nsec delay between the β and the γ emissions. We say a decay has been observed only when there is both a signal for β particle from the PMT and a signal of the correct energy from the germanium detector for the decay emissions of ^{239}Np , ^{233}Pa , and ^{42}K .

2.3.1 Shielding

To reduce ambient background radiation, we shield the sample, PMT and Ge detector with Pb and Cu. 4 inches of Pb will reduce 1 MeV gamma rays by a factor of 3200 and 2 MeV gamma rays by a factor of 175. This is sufficient for our purposes. Greater thickness will provide additional attenuation of gamma rays, but it also increases the probability of undesired cosmic-ray interaction within the shielding, thereby generating more background radiation in the detector area. 2 inches of Cu will reduce the 80 keV x-ray generated from the Pb by a factor of 10^{15} [2].

Chapter 3

Experimental Setup

3.1 Overview

The general setup of the detectors is shown in Figure 3.1. An 20975 cm^3 ($8'' \times 8'' \times 20''$) volume is shielded by $2''$ of Cu on the inside and $4''$ of Pb on the outside. The Ge detector is imbedded in the shielding so that the front of the detector protrudes into the shielded detector chamber. A 665 cm^3 (10cm x 9cm diameter) liquid scintillator container made out of glass and plastic is attached to the PMT. The container and PMT are wrapped in black tape to prevent light leakage. The PMT and scintillator are supported by pieces of copper inside the chamber and placed in front of the germanium detector to maximize the acceptance angle for gamma entry into the detector. One wall of the chamber is removable for the placement and the removal of PMT and samples inside.

3.2 Photomultiplier Tube

The photomultiplier tube (PMT) used in this experiment is a 12-stage photomultiplier tube (model PM2312) from Amperex. It is a 68 mm useful diameter head-on photomultiplier tube with a planoconcave window and a semi-transparent bialkaline type D photocathode. The tubes are intended for use in nuclear physics where the number of pho-

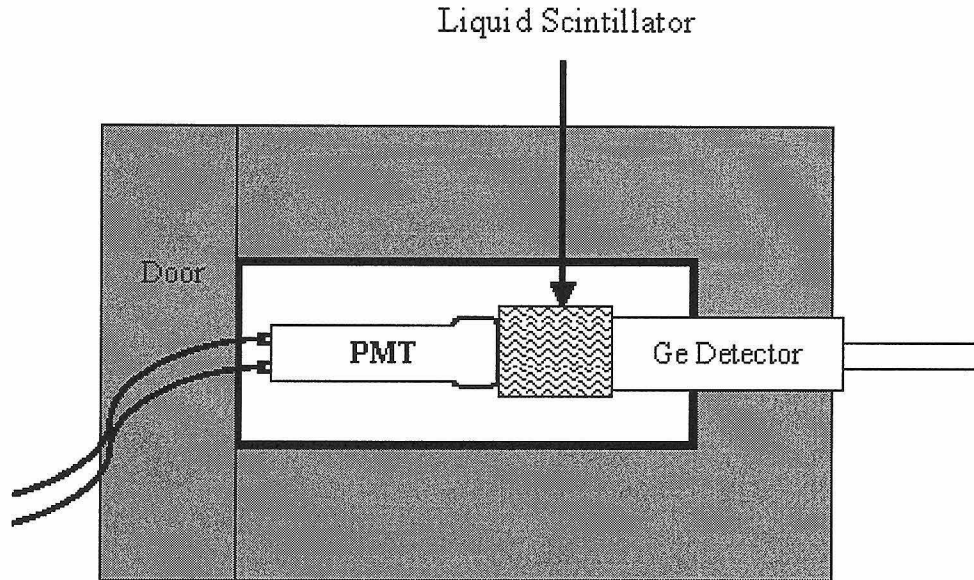


Figure 3.1: schematic of the coincidence setup

tons to be detected is very low and where good time characteristics and a good linearity are required. The supply voltage is 1500 V.

3.3 High Purity Germanium Photon Detector

An EG&G ORTEC p-Type High Purity Germanium Photon Detector is used to measure gamma emissions in the coincidence setup. The detector is attached to a liquid nitrogen dewar for cryogenic cooling. The detector is supplied with a positive 4000 V bias from an ORTEC High Voltage Supply. A pulser running at 100 Hz is connected to the test input of the Ge detector serves as a live time counter for the coincidence detection. The relative efficiency at 1332 keV ^{60}Co line is 80% of a standard NaI detector according to the detector specification.

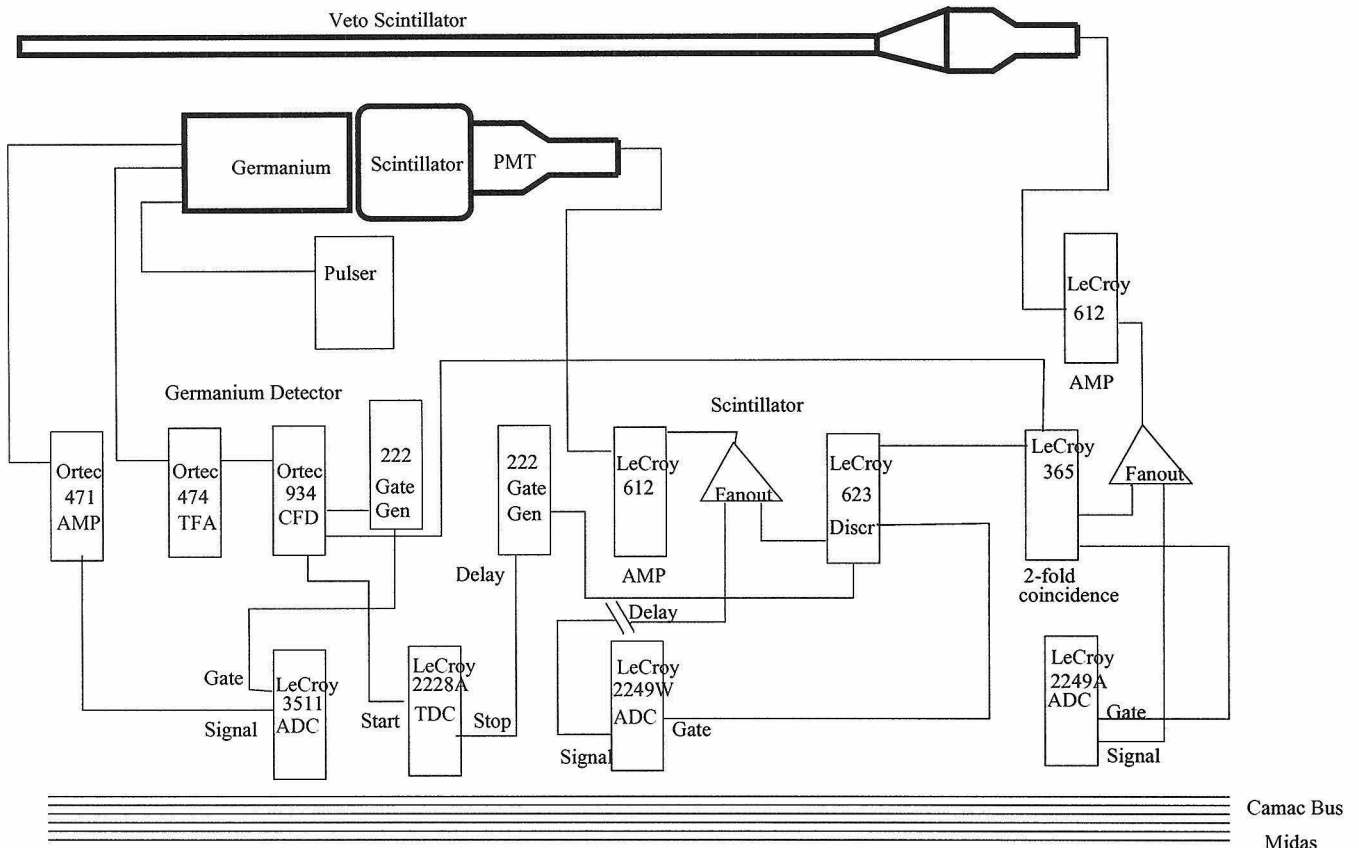


Figure 3.2: Electronics Diagram

3.4 Electronics

The electronics used to record the detector signals are connected according to the diagram shown in Figure 3.2. The HPGe detector signal is sent to the ORTEC 471 Amplifier and the amplified signal is received by the LeCroy 3511 Analog-to-Digital Converter (ADC). A second output signal is sent from the HPGe detector to the ORTEC 474 Time-Filtering Amplifier(TFA), and the output is connected to an ORTEC 934 Constant Fraction Discriminator(CFD). One output goes to a gate generator to provide the 3511 ADC with a gate. The 3511 peak sensing ADC integrates the HPGe signal and converts it into a 13-bit digital number. A second signal from the CFD initiates the Time-to-Digital Converter(TDC). The TDC continues to count until a signal from a gate generated by a PMT signal arrives, or when its range is exceeded. The PMT signal is amplified by a LeCroy 612 Amplifier before it is split into two paths. One path goes to the discriminator to produce a gate for the LeCroy

2249W ADC, while the other goes through nanosecond delays so that both the signal and the gate arrive at the 2249W ADC at the same time. The 2249W ADC is charge sensing and it digitizes data to 11 bits. Whenever a signal arrives at either the 3511 ADC from the HPGe detector or the 2249W ADC from the PMT, both ADC values and the TDC value are recorded by the data acquisition system.

3.5 Data Acquisition

A Hytec 1331 CAMAC controller interfaced with the ADCs is responsible for reading out the digital data. The controller is connected to a IBM compatible PC card on an 500 MHz Pentium III processor running Linux. The data acquisition is managed by the software MIDAS version 1.8.0, developed by TRIUMF [3]. The data analysis is performed using the high energy physics software packages PAW and ROOT [4].

Chapter 4

Data Analysis

4.1 Shielding Effects on the HPGe Detector

A background run was recorded before the shielding was installed. The HPGe spectrum was normalized and compared with another normalized background spectrum taken after the shielding was in place. Figure 4.1 shows that the shielding reduced the background by more than 2 orders of magnitude.

4.2 PMT Calibration from Compton Scattering

Compton scattering is the dominating process for determining the energy of the photons deposited in the PMT because the scintillator has a $Z=2.7$ (for CH_2). Calibration data were obtained using the radioactive sources ^{22}Na , ^{54}Mn , ^{57}Co , ^{137}Cs , and ^{133}Ba . These sources provided monoenergetic photons between 81 keV and 1275 keV for our measurements. They were placed between the scintillator container and the Ge detector. β particles with energy between 100 keV and 1500 keV could not penetrate the 0.5 cm of glass and plastic surrounding the liquid scintillator[5], we only observe the compton scattering of photons from sources outside the scintillator volume. The signals from ^{57}Co γ emissions were too low to distinguish from the noise, therefore they were excluded in the data set. The event counts per bin were integrated over every 32 bins to smooth the spectrum for this analysis.

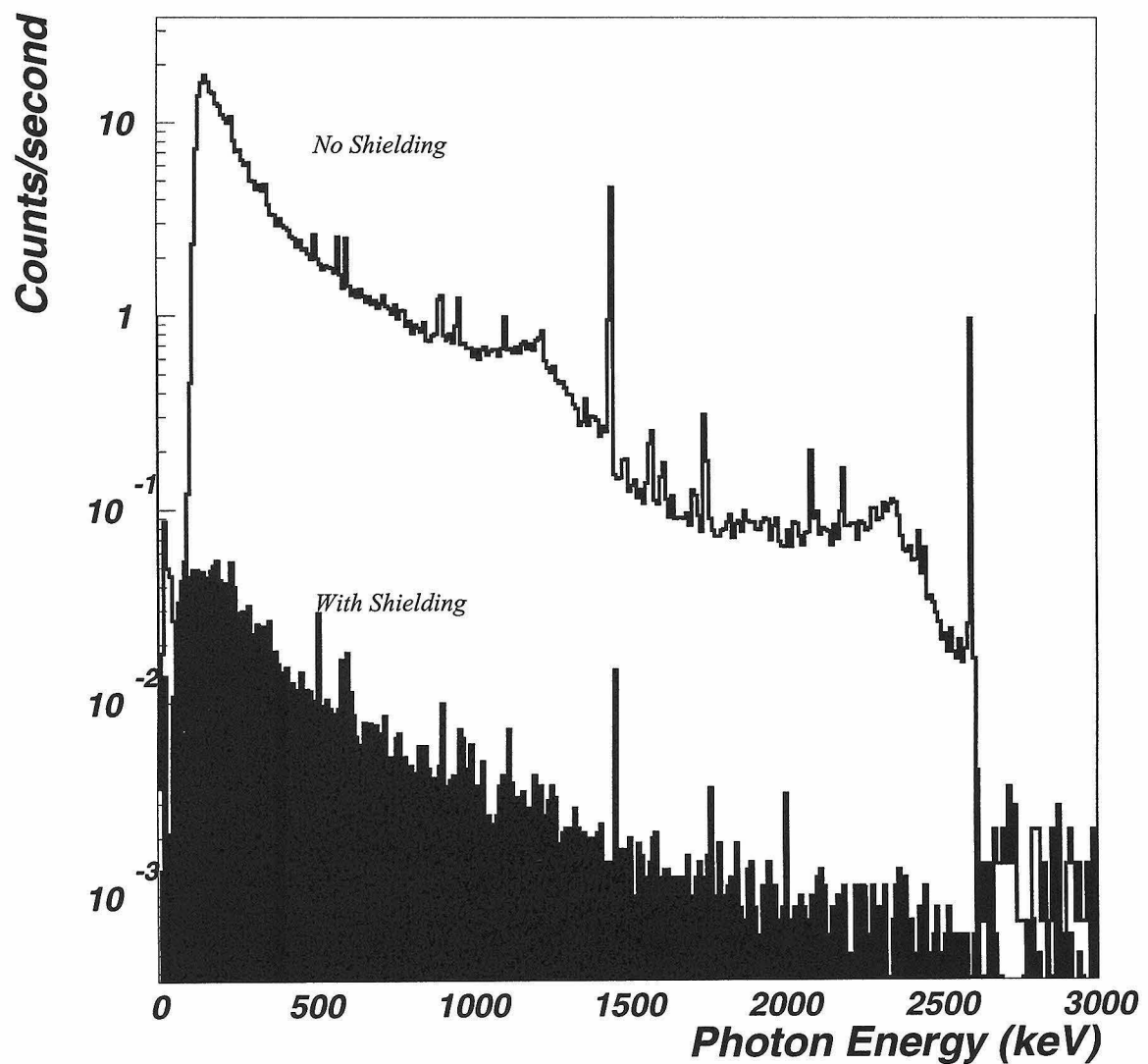


Figure 4.1: HPGe Spectra - before and after shielding

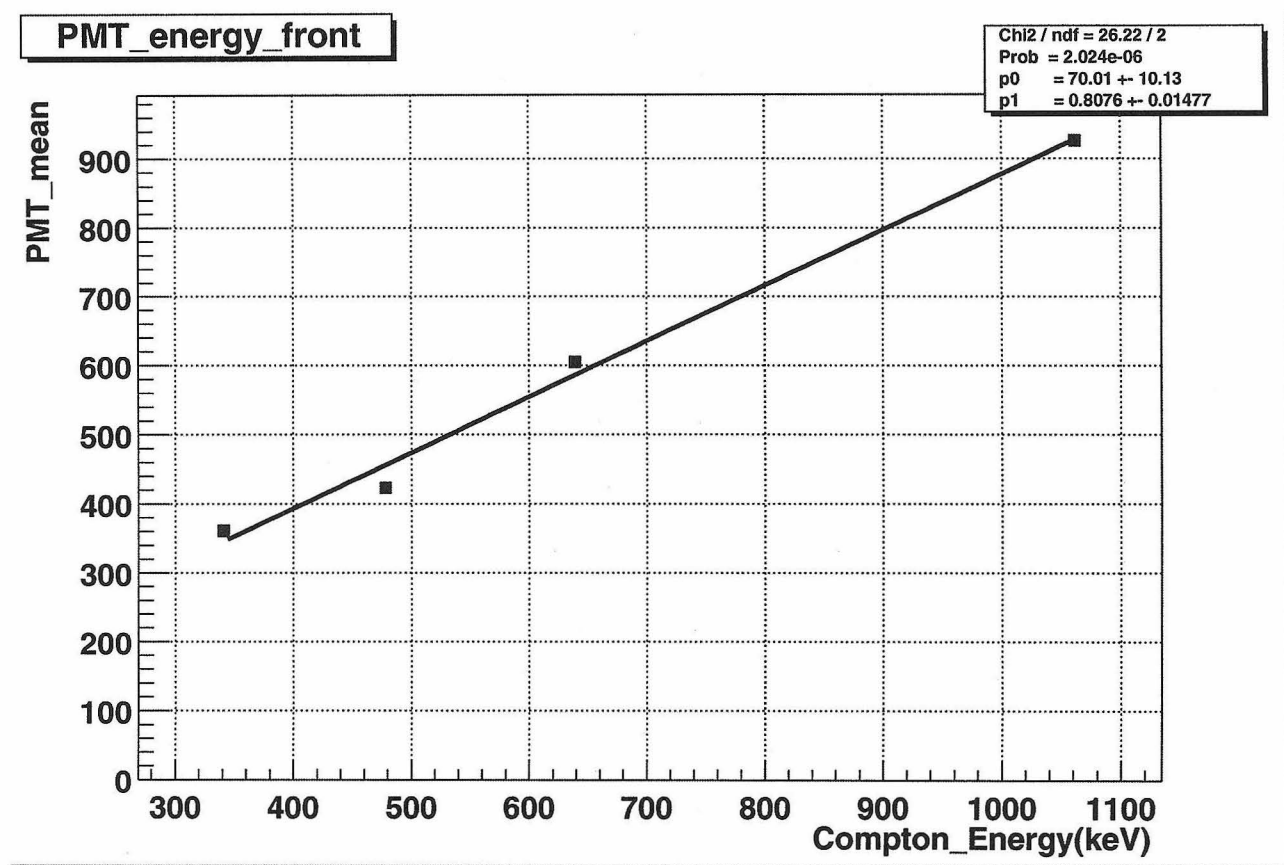


Figure 4.2: PMT peak vs. Compton energy

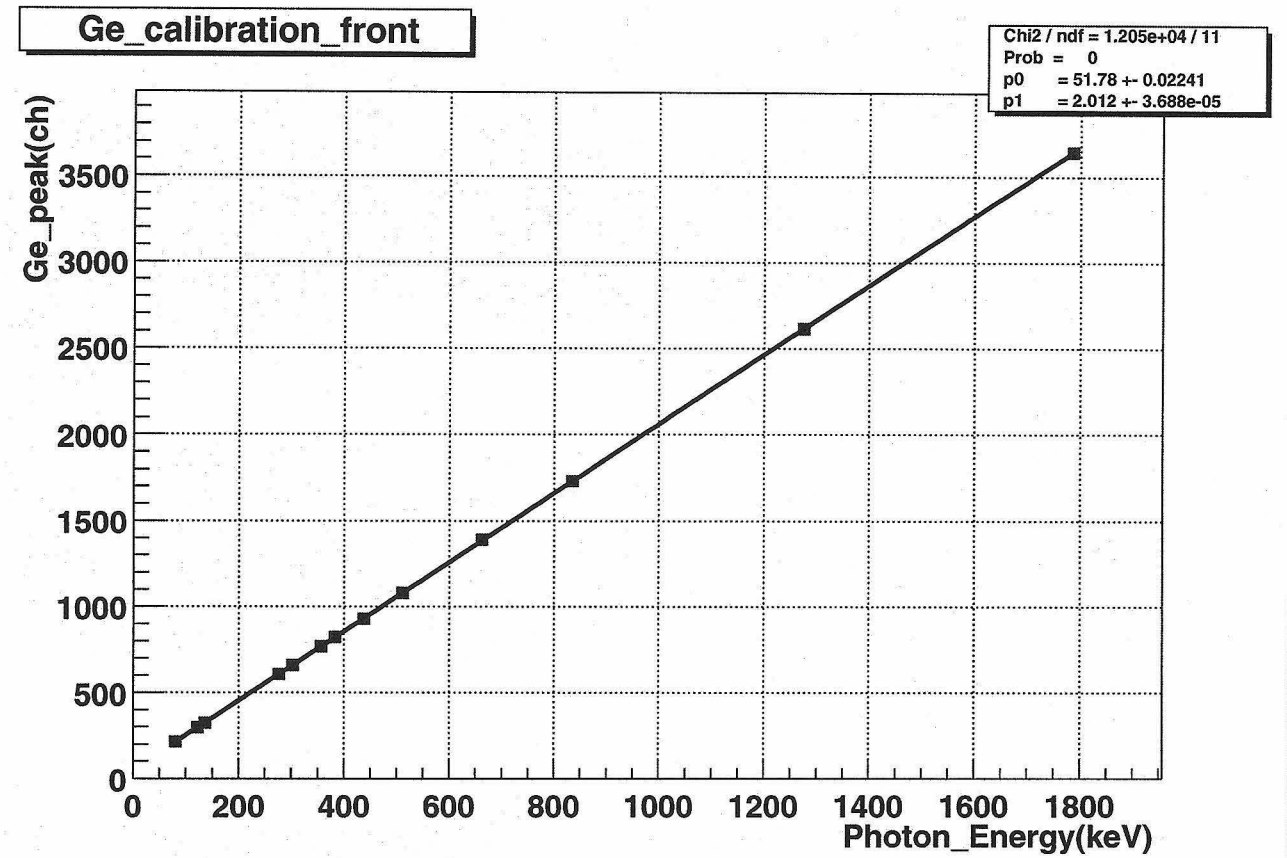


Figure 4.3: HPGe Detector Calibration Plot

The slope was calculated by taking the difference between consecutive 32 bins. A gaussian was fit around the peak where the slope is most negative to determine the compton energy. The slope of the PMT readout with respect to the energy is 0.8076 ± 0.01477 channels/keV, with a pedestal of 70.01 ± 10.13 channels.

4.3 HPGe Detector Calibration

The photoelectric effect is the dominating process that determines the energy of the photons deposited in the HPGe detector because Ge has a Z=32. HPGe detector calibration

data was obtained from the same runs as the PMT calibration data. Figure 4.2 shows the plot of energy vs. peak channel in the HPGe detector spectrum. The corresponding channel with respect to the energy of the photon is

$$Channel = (2.012 \pm 0.002042) \times Energy + (49.64 \pm 1.445).$$

4.4 HPGe Detector Resolution

According to the HPGe detector specification, the FWHM of the peak at 1332 keV from ^{60}Co emission should be 2.10 keV or less. Our own tests showed that at 1332 keV (channel 2730), the FWHM is 3.78 ch, which corresponds to 1.88 keV. The plot is shown in Figure 4.4.

4.5 Efficiency of the HPGe detector

The set of calibration runs for the PMT and Ge detector was used to determine the efficiency of the Ge detector when the source is between the scintillator and the Ge detector. Another set of data was taken with the sources next to the scintillator on top of the PMT. The Ge crystal of the detector is 3.6 cm in diameter with a 0.5 cm aluminum casing. The scintillator container is 10 cm deep. The radius of the PMT is 3.8 cm. The efficiency of the Ge detector is dependent on the acceptance angle $G(x,y)$ and the attenuation factor $A(x,y)$. We let the origin be the center of the front of the detector casing.

$$\epsilon(x,y) = \epsilon_0 G(x,y) A(x,y)$$

We want to calculate the efficiency of the Ge detector for a source in the center of the container, at distance $x=L/2$ and $y=0$ where L is the length of the scintillator container.

$$\epsilon(L/2, 0) = \epsilon_0 G(L/2, 0) A(L/2, 0),$$

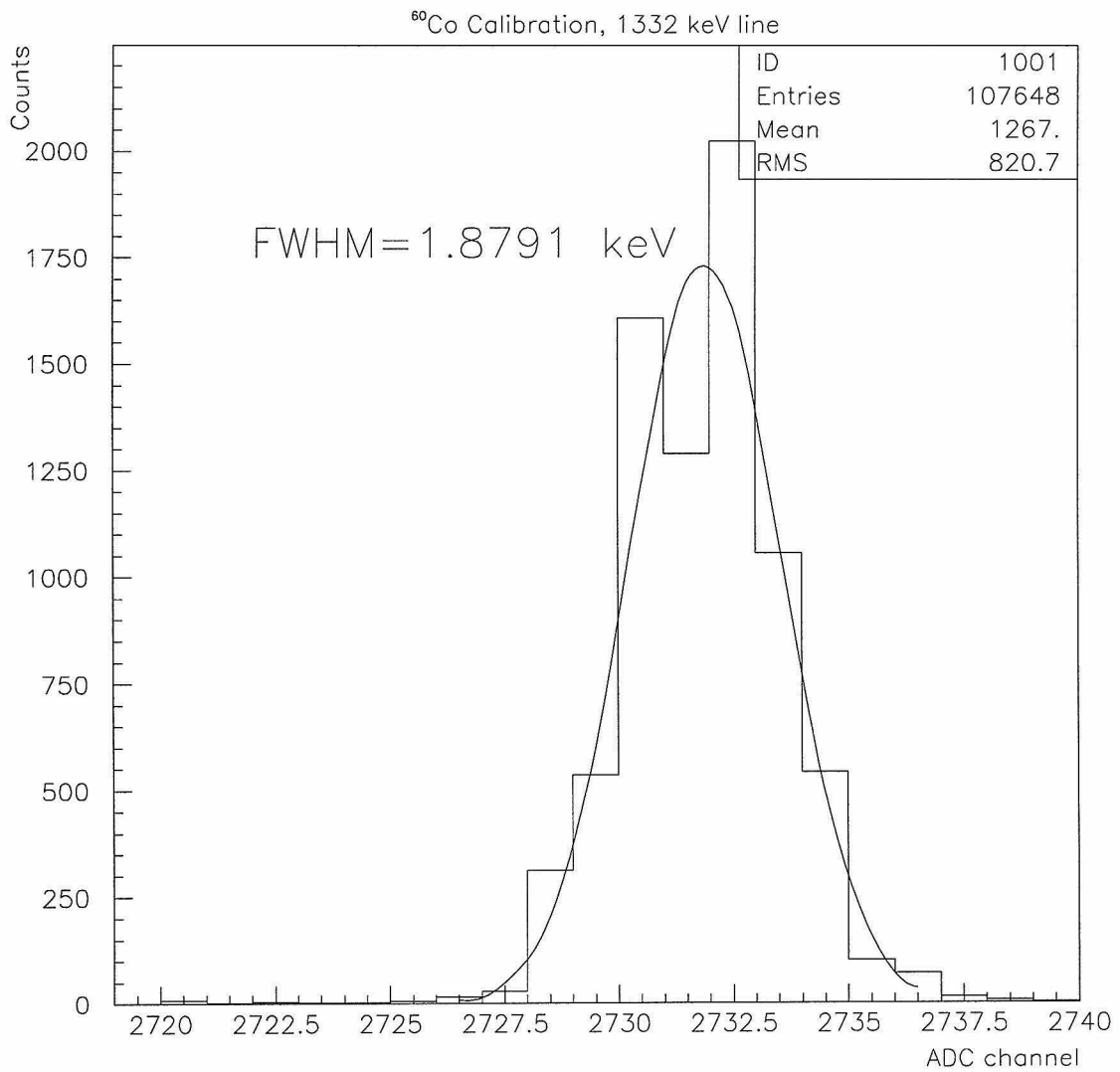


Figure 4.4: HPGe Detector Resolution Spectrum at 1332 keV

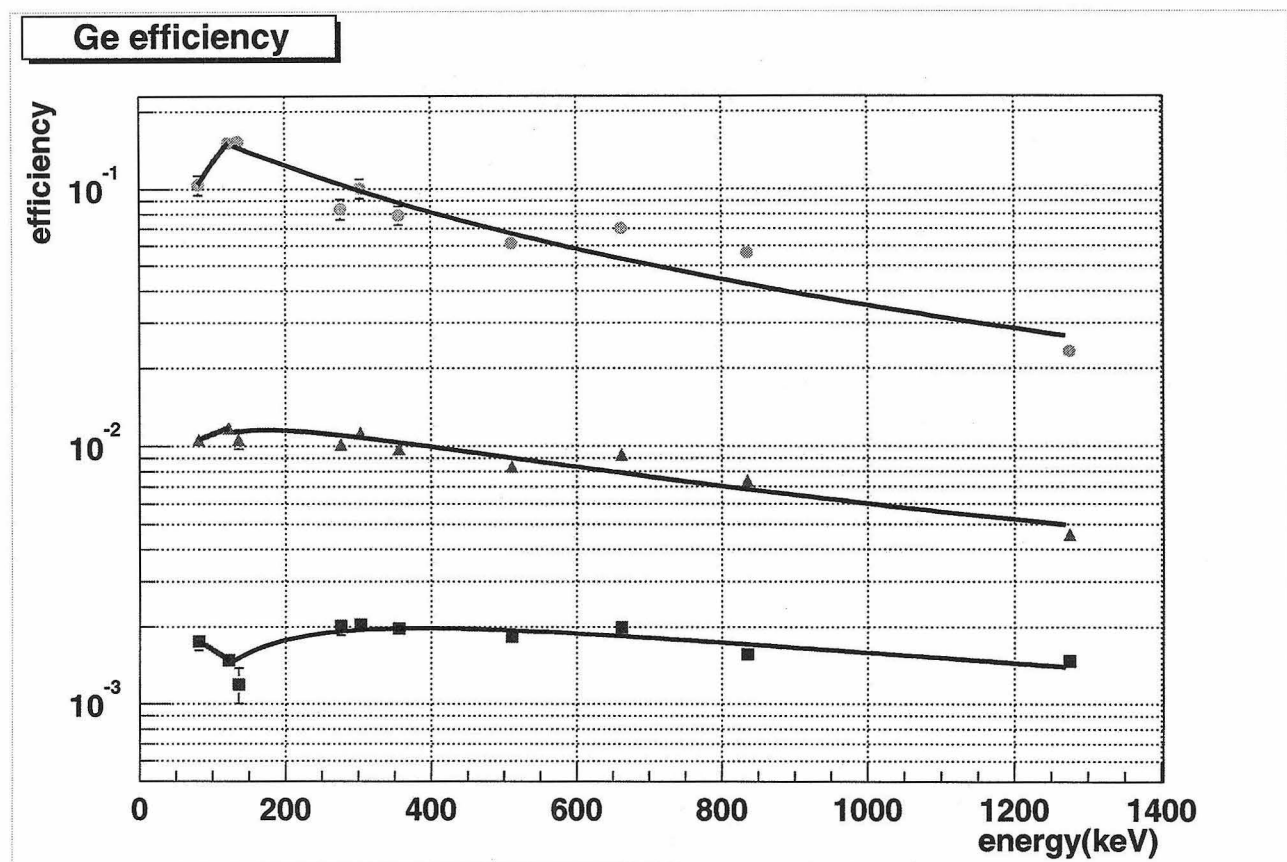


Figure 4.5: Plot of energy vs. efficiency of the Ge detector. \circ front; \square back; \triangle center (extrapolated).

where

$$\epsilon_0 = \frac{\epsilon(0)}{G(0, 0)A(0, 0)}.$$

The attenuation factor looks like

$$A(x, y) = e^{-\alpha\sqrt{x^2+y^2}}.$$

Therefore

$$\epsilon(L/2, 0) = \epsilon_0 G(L/2, 0) e^{-\alpha L/2} = \epsilon_0 G(L/2, 0) \left(\frac{\epsilon(L, 3.8)}{G(L, 3.8)\epsilon_0} \right)^{L/(2\sqrt{L^2+3.8^2})}.$$

We fit the data to a typical efficiency function for Ge detectors (Figure 4.5) and obtained the result:

$$\ln(\epsilon) = (-10.15 \pm 0.13) + (2.206 \pm 0.039) \ln E + (-0.2137 \pm 0.0036)(\ln E)^2,$$

where E is the energy.

However, the efficiency at low energy (below 100 keV) actually decreases due to attenuation in the aluminum casing surrounding the HPGe detector. Since we do not have enough data points near the 100 keV region where we expect to see the peak efficiency, we use a linear function determined by the 81 keV emission from ^{133}Ba and the 122 keV emission from ^{57}Co . So for $E < 122$ keV,

$$\epsilon = (8.336 \pm 2.102) \times 10^{-3} + (2.815 \pm 1.956) \times 10^{-5} E.$$

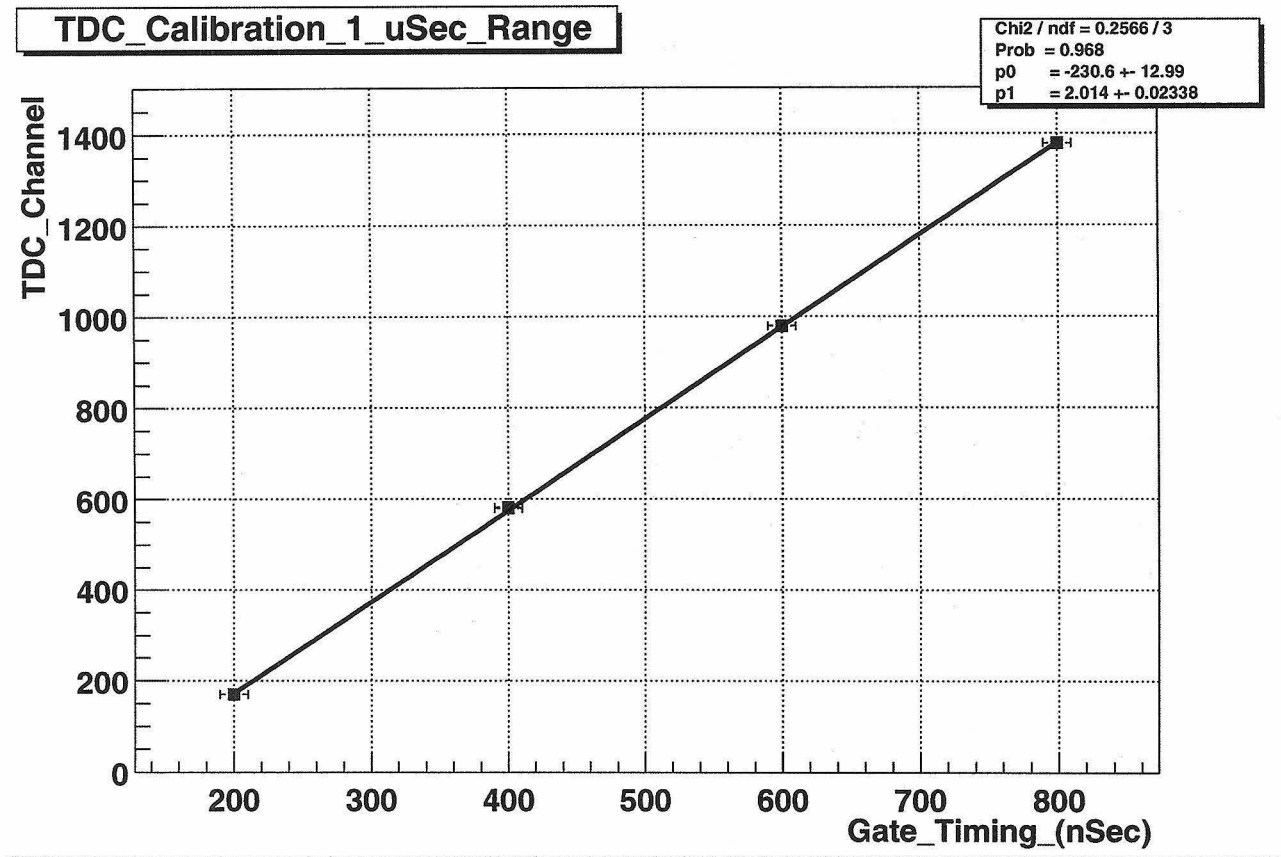


Figure 4.6: TDC Calibration for 1 μ sec full scale time range

4.6 TDC Calibration

The LeCroy 2228A High Precision Time-to-Digital Converter has 3 switch-selectable options for full scale time range of 1 μ sec, 2 μ sec, and 10 μ sec. Calibration data were taken using a gate generator with an adjustable delay. The leading edge triggered the TDC start, and a short delayed pulse at the end of the first gate triggered the TDC stop. The results for each of the full scale time range settings are plotted on Figure 4.6 - 4.8. The slopes of the TDC channels are listed below:

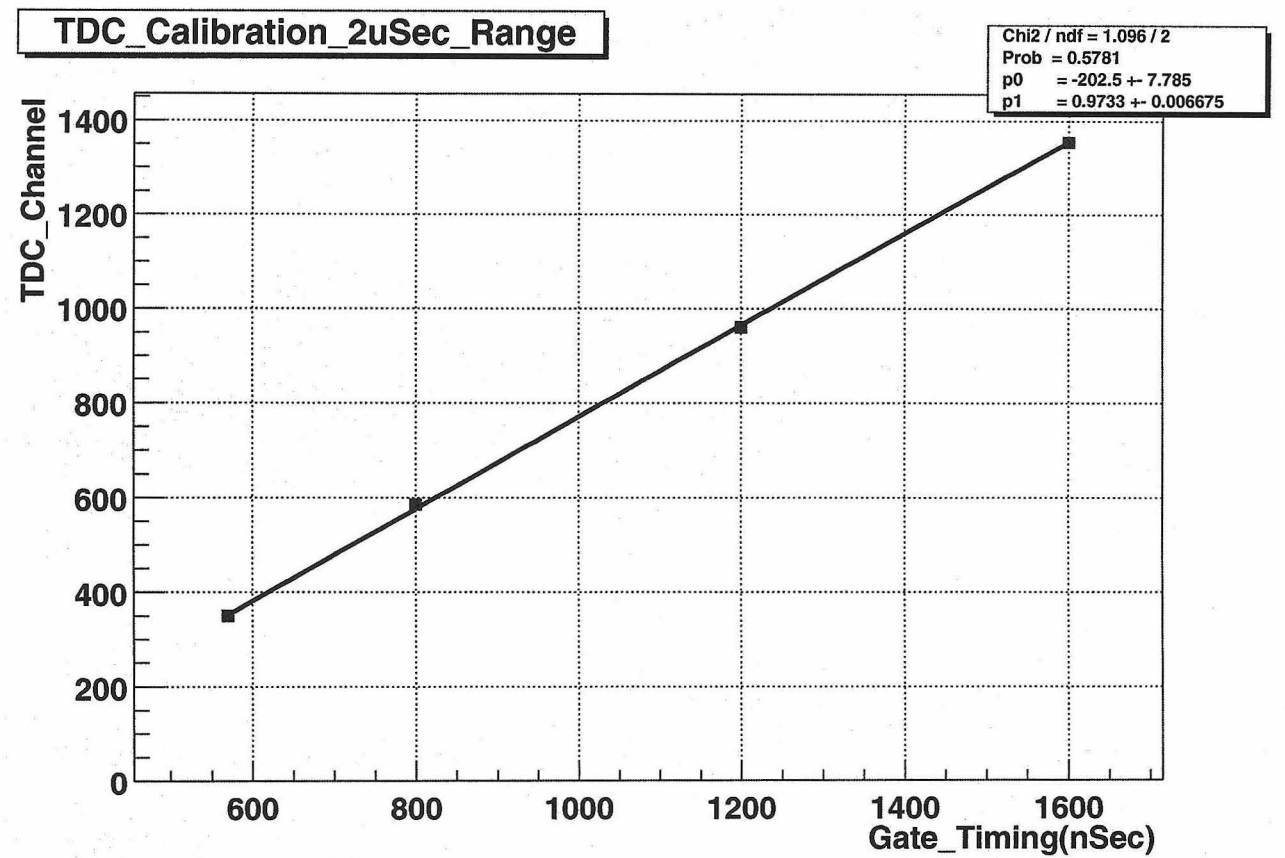


Figure 4.7: TDC Calibration for 2 μ sec full scale time range

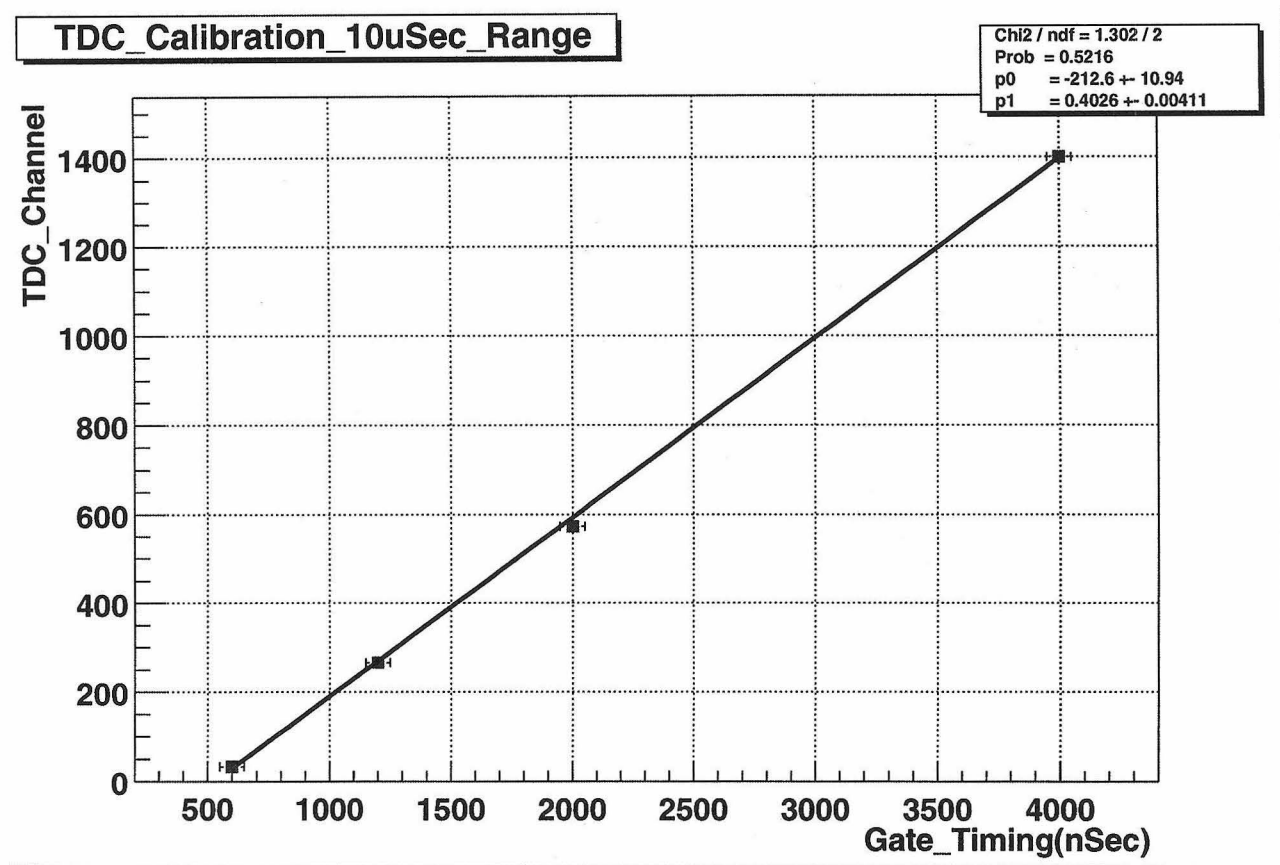


Figure 4.8: TDC Calibration for $10 \mu\text{sec}$ full scale time range

full scale time range	$\frac{d}{dt}$ (channels/nsec)
1 μ sec	2.014 ± 0.023
2 μ sec	0.9733 ± 0.0067
10 μ sec	0.4026 ± 0.0041

For our purposes, we choose the 2 μ sec setting because it is most appropriate for our time scale. Since there is a slight delay between the HPGe detector signal and the PMT signal, simultaneity for the two detectors is defined by the peak in the TDC spectrum when the simultaneous emission of a β particle and a γ particle is registered in both detectors. We should also be able to observe the 192 nsec delay between the β emission and the γ emission in ^{239}Np decay.

4.7 Na Coincidence Measurement

^{22}Na undergoes beta decay either by positron emission or by electron capture, and then it emits a gamma ray with an energy of 1275 keV. We use a ^{22}Na source to evaluate the efficiency of our coincidence detection. The counting rates are given by the formulas:

$$R_{Ge} = A\epsilon_{Ge},$$

$$R_{PMT} = A\epsilon_{PMT},$$

$$R_{coincidence} = A\epsilon_{Ge}\epsilon_{PMT},$$

where A is the activity of the source and ϵ is the efficiency of the detector. We can extract the activity by multiplying the counting rates of the PMT and the Ge detector and divide by the coincidence rate.

$$\frac{R_{Ge}R_{PMT}}{R_{coincidence}} = \frac{A\epsilon_{Ge}A\epsilon_{PMT}}{A\epsilon_{Ge}\epsilon_{PMT}} = A.$$

Figure 4.9 shows the singles spectrum for the PMT and Ge detector, and the TDC coincidence spectrum. A cut at channel 500 was applied to the PMT spectrum so that the peak from the Compton scattering of the 511 keV photons was excluded. A cut around the 511 keV peak was also applied to the Ge spectrum. When both cuts were applied, the only

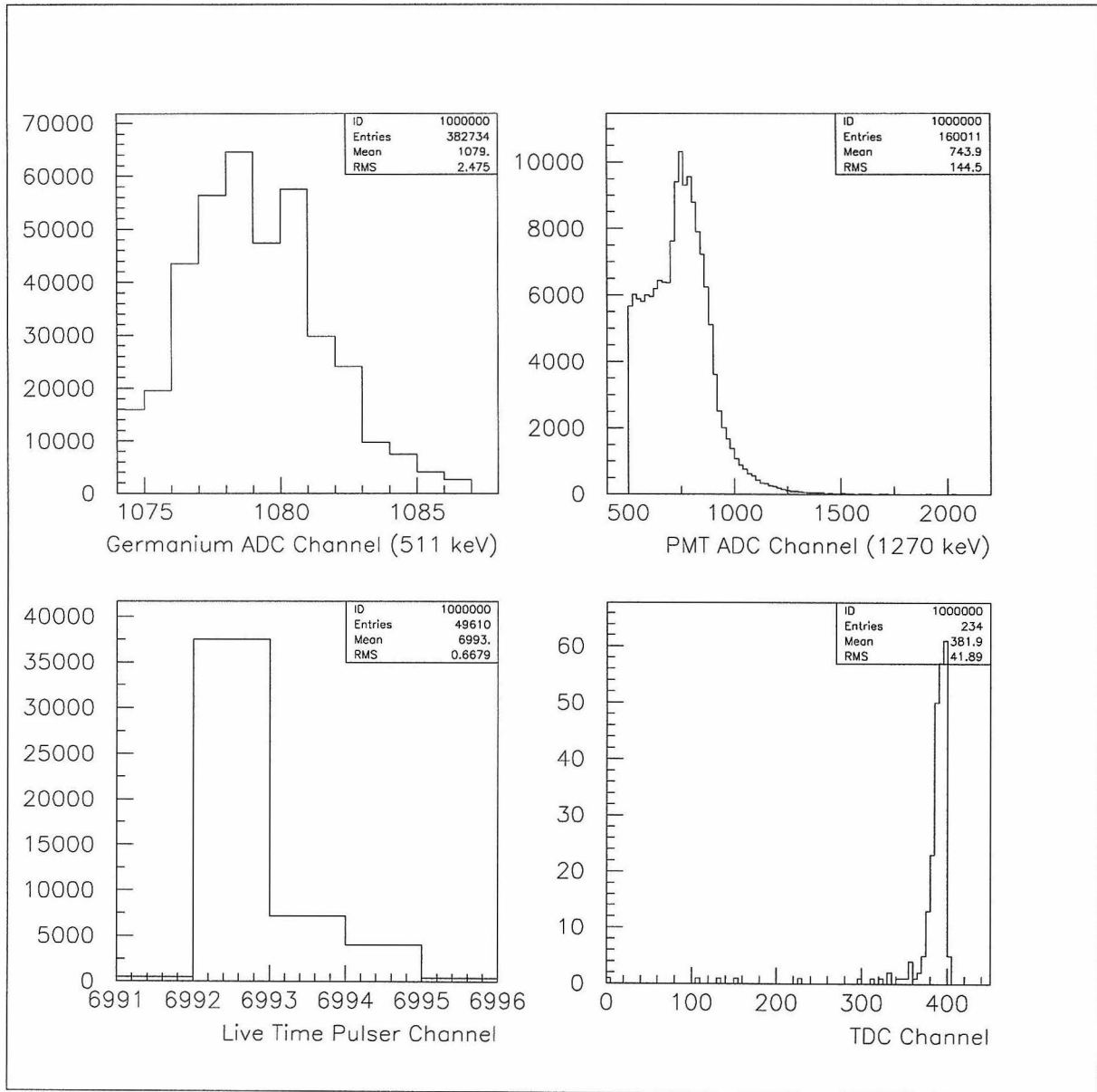


Figure 4.9: Na Coincidence. Top left: HPGe spectrum around the 511 keV peak. Top right: PMT spectrum with a cut at channel 500. Bottom left: live time pulser count. Bottom right: TDC spectrum with cuts in TDC, PMT and HPGe detector spectra.

remaining events were when a 1275 keV photon was observed in the PMT and a 511 keV photon from the annihilation of the beta particle was observed in the Ge detector simultaneously. A cut was also placed on the TDC spectrum so that it excluded the events where the time difference between the two signals exceeded the tolerance for a coincidence. From the data we calculated the activity of the ^{22}Na source to be $0.1426 \pm 0.0094 \mu\text{Ci}$. This agrees with the actual activity $0.1519 \pm 0.0076 \mu\text{Ci}$ within 6.5%, or 0.8σ .

4.8 Expected Background Counts

The background for measurements of radioactive decay is determined by the number of coincidences we observe at the emission energy. Fig 4.10 - 4.12 show the number of coincidences in the PMT and HPGe detector measurements of ^{239}Np , ^{233}Pa , and ^{42}K decays that were recorded in a 4 hour period with 53% live time. The results show that there were either no coincidences, or the TDC value was 0, which we reject because the TDC was set to register an actual value (around channel 400) in a true coincidence event.

One way to estimate the background for measuring ^{239}Np , ^{233}Pa , and ^{42}K decays is to take the probability that the HPGe detects a photon with the emission energy, and multiply it by the probability that a PMT signal arrives within a time window Δt immediately afterwards.

$$R_{\text{coincidence}} = R_{\text{Ge}} \times R_{\text{PMT}} \times \Delta t.$$

We place a time window of $\Delta t = 1 \mu\text{sec}$, and assume we measure the sample for 4 days. The expected background counts are listed below:

	^{239}Np	^{233}Pa	^{42}K
γ emission energy	106 keV	312 keV	1525 keV
estimated background counts in 4 days	7.5×10^{-3}	3.9×10^{-3}	8.7×10^{-5}

If we take a more conservative estimate of the background and assume that 1 ± 1 event had been measured during the background run, we would expect to measure 45 ± 6.7 events in 96 hours, assuming the detectors have 100% live times. However, we would

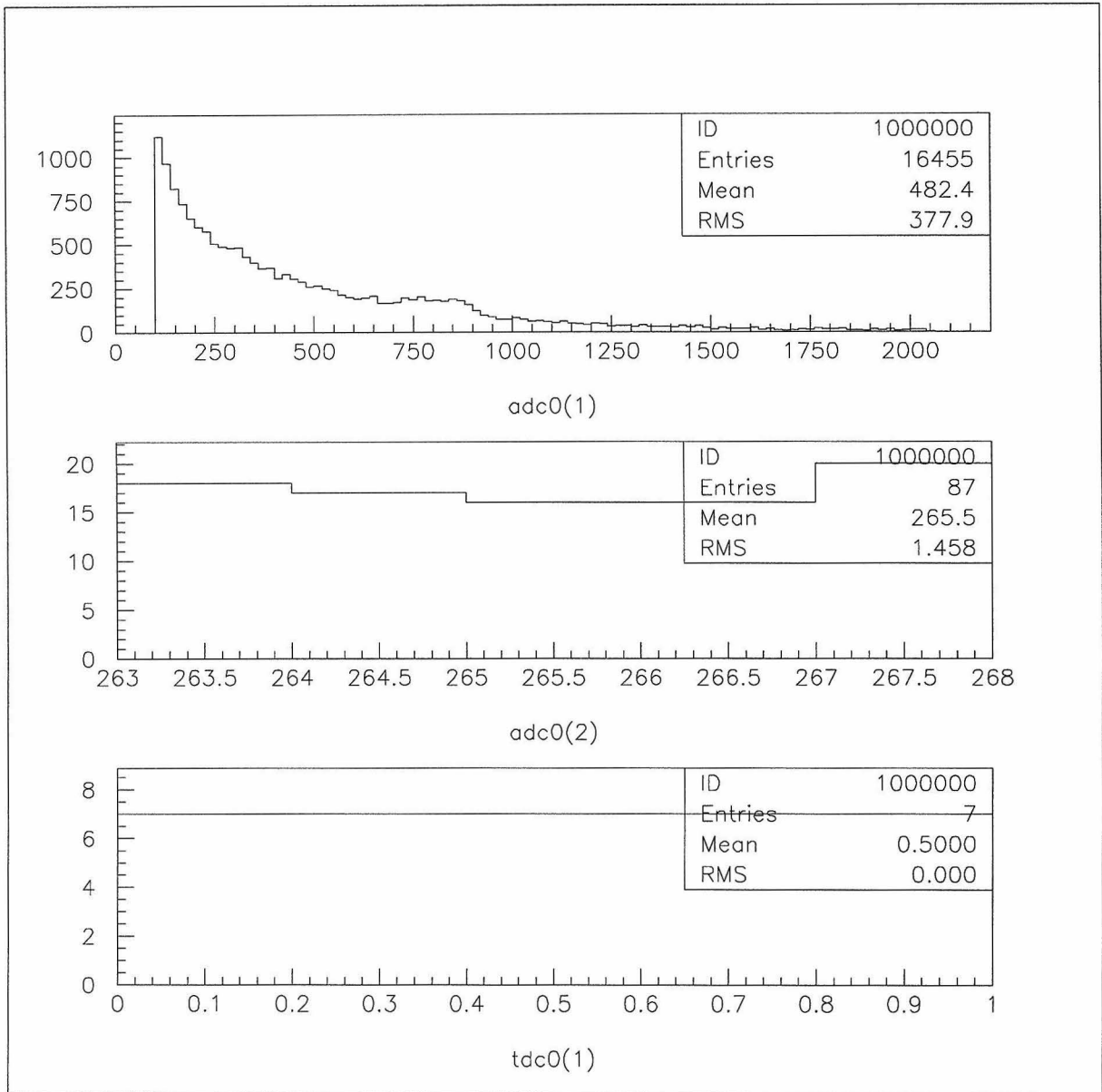


Figure 4.10: Background counts for ^{239}Np 106 keV photon emission. Top: the singles spectra from the PMT with a cut at channel 100 to disregard the noise at lower energies. Middle: the singles spectra from the Ge detector around the energy peaks. Bottom: the TDC counts for the coincidences (when both cuts are applied).

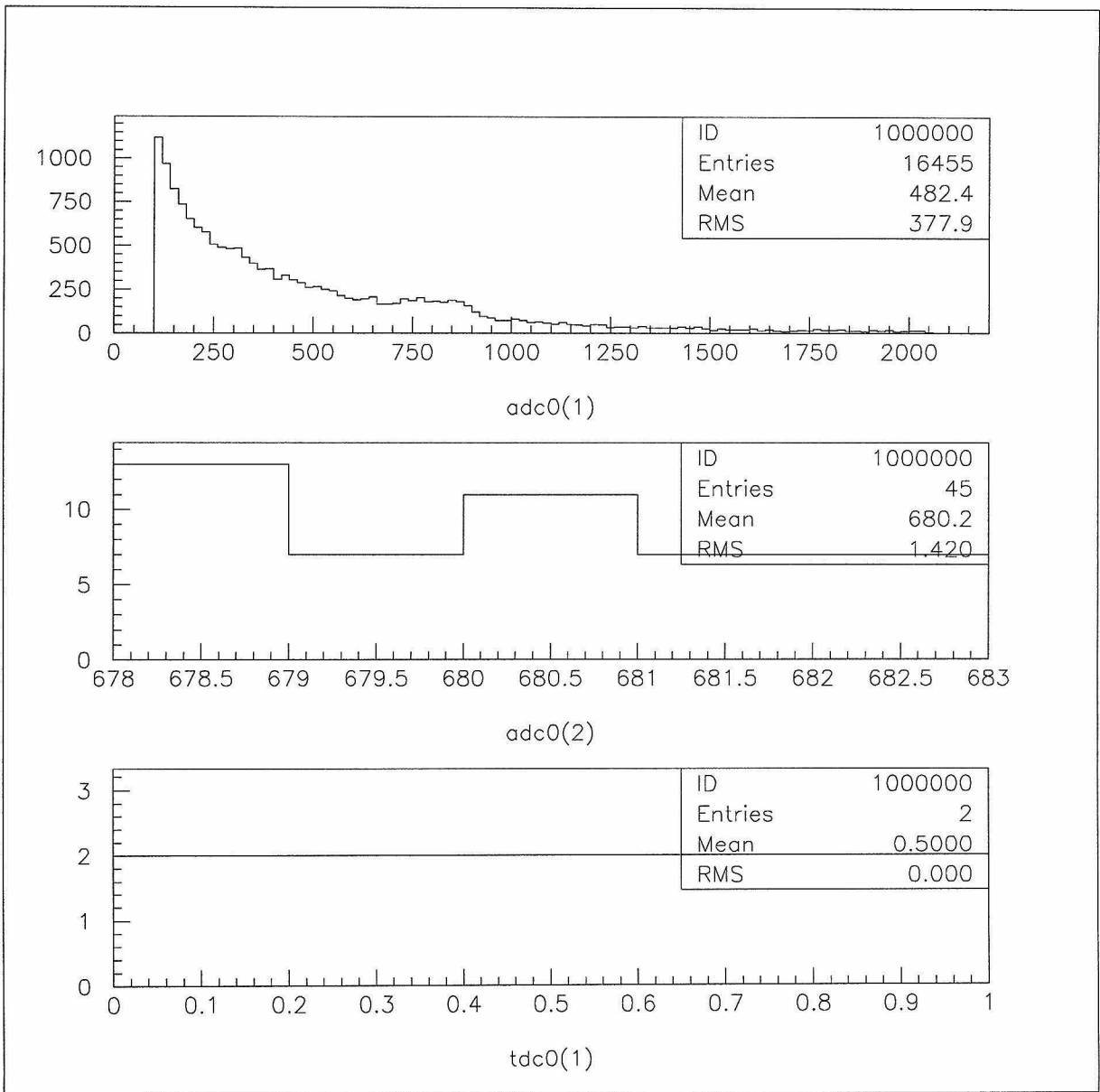


Figure 4.11: Background counts for ^{233}Pa 312 keV photon emission. Top: the singles spectra from the PMT with a cut at channel 100 to disregard the noise at lower energies. Middle: the singles spectra from the Ge detector around the energy peaks. Bottom: the TDC counts for the coincidences (when both cuts are applied).

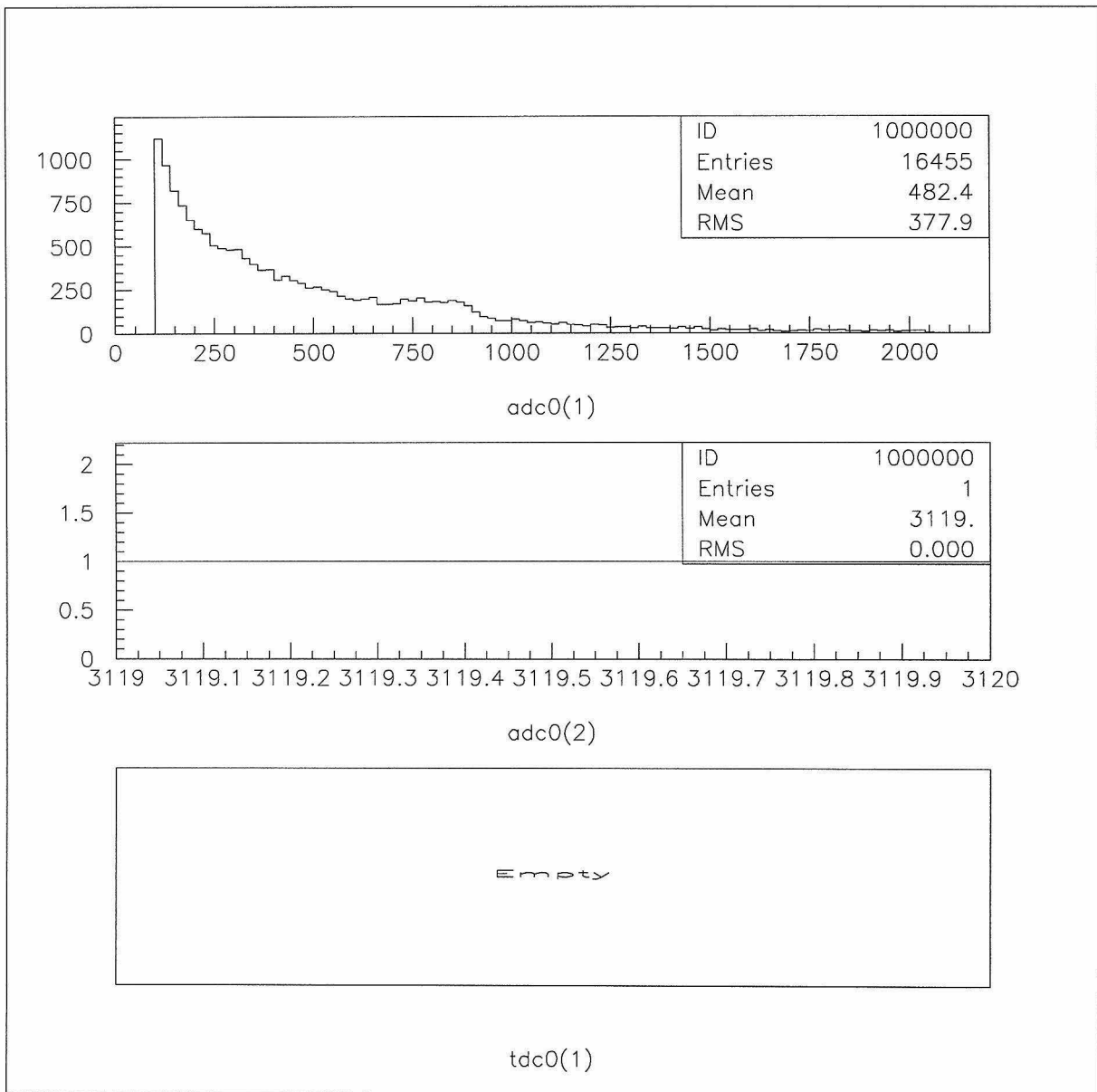


Figure 4.12: Background counts for ^{42}K 1525 keV photon emission. Top: the singles spectra from the PMT with a cut at channel 100 to disregard the noise at lower energies. Middle: the singles spectra from the Ge detector around the energy peaks. Bottom: the TDC counts for the coincidences (when both cuts are applied).

expect to see more background in an actual sample due to source related activities, which we currently have no estimates for. It would require a test run with an activated sample to determine what other isotopes in the source would be activated and how much background they would contribute.

Chapter 5

Results and Conclusion

5.1 Expected Counting Rate

Assuming the sample volume is 250 cm^3 , the expected event rate for ^{238}U , ^{232}Th , ^{40}K can be computed using the formula

$$R = \frac{N\sigma\phi}{\lambda}(1 - \exp -\lambda t_0)(\exp -\lambda t_1)(1 - \exp -\lambda t_2)\epsilon,$$

where

N = number of atoms

= mass of sample \times density of scintillator \times concentration $\times 6.02 \times 10^{23}$ /atomic mass,

σ = capture cross section,

ϕ = n-flux = $8 \times 10^{13} \text{ n/cm}^2\text{s}$,

λ = decay rate = $\ln 2 / \tau_{1/2}$,

t_0 = irradiation time = 100 hours,

t_1 = preparation time before measurement = 48 hours,

t_2 = counting time = 96 hours,

ϵ = counting efficiency = $\epsilon_{Ge} \times \epsilon_{PMT}$.

The counting efficiency is computed using the HPGe efficiency curve from section 4.4

and assuming PMT efficiency to be 50%. We also assume that the live time of the detector is 100%. The expected counting rate from each of the three elements are:

element	^{238}U	^{232}Th	^{40}K
number of atoms in sample	5.31×10^9	5.45×10^9	3.16×10^{10}
actual decay element	^{239}Np	^{233}Pa	^{42}K
photon energy	106 keV	312 keV	1525 keV
capture cross section	2.75 barns	7.31 barns	1.46 barns
decay rate (hour $^{-1}$)	1.23×10^{-2}	1.07×10^{-3}	5.59×10^{-2}
HPGe efficiency	(1.132 ± 0.295) $\times 10^{-2}$	(1.074 ± 0.3061) $\times 10^{-2}$	(4.227 ± 1.559) $\times 10^{-3}$
total number of counts in 4 days	526 ± 137	542 ± 154	$(3.322 \pm 1.225) \times 10^5$

5.2 Sensitivity of the Coincidence Setup

We take the conservative estimate of the background from section 4.8 and assume that we measure exactly 45 events in 96 hours. Then the number of decays observed from the sample after subtracting the background is

$$N_{sample} = N_{total} - N_{background} = 0 \pm 9.5.$$

Therefore we need to measure at least 19 events in addition to the background to obtain a non-zero event at 95% confidence level. The sensitivity is the minimal concentration at which the coincidence setup can measure 19 events in 96 hours. This can be calculated from the formula in section 5.1. The results are in the table below:

isotope	^{238}U	^{232}Th	^{40}K
concentration	4×10^{-16} g/g	4×10^{-16} g/g	6×10^{-19} g/g

5.3 Future Improvements

Since conducting the data collection for this experiment, we have found and removed the background process on the computer that had reduced the data recording rate. Currently the detectors are running at greater than 99% live time at 1 kHz event rate. There are other modifications that can be made to improve the performance of the coincidence setup. High energy muons passing through the detector can scatter off the Pb or Cu and produce photons by bremstrahlung. The Pb and Cu can also absorb muons and make neutrons which can penetrate the entire shield. We have prepared a photomultiplier tube designed for cosmic ray muon detection. Its surface is large enough to cover the top of the detector chamber, and it can be used to veto false coincidence events generated by cosmic ray muons.

Another source of background in the setup is contamination from the PMT. A careful selection of PMT for low radioactivity should further reduce the background. Other contaminations can be removed by cleaning the detector chamber carefully, and also by sealing the chamber and filling it with inert gas to reduce airborne contamination.

5.4 Conclusion

A coincidence setup has been designed and built for coincidence detection of neutron activated nuclei. It has a sensitivity of 4×10^{-16} g/g, 4×10^{-16} g/g, and 6×10^{-19} g/g for ^{238}U , ^{232}Th , and ^{40}K , respectively. This is sufficient for measuring the radiopurity of the liquid scintillator at KamLAND. An addition of a cosmic muon veto and removal of radioactive contamination from inside the detector chamber should reduce the background further.

Bibliography

- [1] *Proposal for US Participation in KamLAND*. March 1999.
- [2] *Modular Pulse-Processing Electronics and Semiconductor Radiation Detectors*. EG&G ORTEC, 1997-98.
- [3] <http://midas.triumf.ca>
- [4] <http://root.cern.ch>
- [5] Greeniaus, L. G. ed. *TRIUMF Kinematics Handbook*. 2nd ed. September 1987.
- [6] Knoll, Glenn. *Radiation Detection and Measurement*. 2nd ed. New York: John Wiley & Sons, 1989.